Published in final edited form as:
J Med Chem. 2012 March 8; 55(5): 2416–2426. doi:10.1021/jm201713h.

Development of *Toxoplasma gondii* Calcium-Dependent Protein Kinase 1 (*Tg*CDPK1) Inhibitors with Potent Anti-*Toxoplasma* Activity

Steven M. Johnson[1], **Ryan C. Murphy**[1], **Jennifer A. Geiger**[4], **Amy E. DeRocher**[4], **Zhongsheng Zhang**[3], **Kayode K. Ojo**[2], **Eric T. Larson**[3], **B. Gayani K. Perera**[1], **Edward J. Dale**[1], **Panqing He**[2], **Molly C. Reid**[2], **Anna M.W. Fox**[2], **Natascha R. Mueller**[2], **Ethan A. Merritt**[3], **Erkang Fan**[3], **Marilyn Parsons**[4,5], **Wesley C. Van Voorhis**[2,5,*], and **Dustin J. Maly**[1,*]

[1]Department of Chemistry, University of Washington, Seattle, Washington, USA

[2]Division of Allergy and Infectious Diseases, Department of Medicine, University of Washington, Seattle, Washington, USA

[3]Department of Biochemistry, University of Washington, Seattle, Washington, USA

[4]Seattle Biomedical Research Institute, Seattle, Washington, USA

[5]Department of Global Health, University of Washington, Seattle, Washington, USA

Abstract

Toxoplasmosis is a disease of prominent health concern that is caused by the protozoan parasite, *Toxoplasma gondii*. Proliferation of *T. gondii* is dependent on its ability to invade host cells, which is mediated, in part, by calcium-dependent protein kinase 1 (CDPK1). We have developed ATP competitive inhibitors of *Tg*CDPK1 that block invasion of parasites into host cells, preventing their proliferation. The presence of a unique glycine gatekeeper residue in *Tg*CDPK1 permits selective inhibition of the parasite enzyme over human kinases. These potent *Tg*CDPK1 inhibitors do not inhibit the growth of human cell lines and represent promising candidates as toxoplasmosis therapeutics.

Introduction

Toxoplasma gondii is a food and waterborne pathogen that can infect humans and all warm-blooded animals.[1, 2] It is acquired by consumption of undercooked meat bearing tissue cysts or by ingesting foods or water contaminated with oocysts shed by infected felines. The oocysts are highly infectious and environmentally stable, making infection by this route a serious concern in areas where the water supply is not safe and secure. During the initial infection, the parasites proliferate rapidly as tachyzoites until controlled by the immune system. At that point, the parasite transforms into the bradyzoite, a slow growing stage, establishing a reservoir of tissue cysts in the brain and other tissues. Periodically, the tissue cysts rupture, releasing tachyzoites that again replicate rapidly. If not brought under control

Correspondence should be addressed to: DJM (Tel: 206-543-1653. Fax 206-685 7002. maly@chem.washington.edu) or WCVV (Tel: 206-543-2447. Fax: 206-616-4898. wesley@uw.edu).

The authors are solely responsible for the content.

Supporting Information:
Tabulation of IC_{50}-fold differences between human kinases and *Tg*CDPK1; graphical comparison of SRC and *Tg*CDPK1 enzymatic IC_{50} results; *Tg* cell proliferation EC_{50} shifts with Gly128Met *Tg*CDPK1 mutant for compounds **15o** and **16n**; synthesis and characterization data for all compounds. This material is available free of charge via the Internet at http://pubs.acs.org.

by the immune system, this can cause re-emergence of the disease. The result in immunocompromised individuals is toxoplasmic encephalitis. In some regions of the world, *T. gondii* infections even appear to be problematic in immunocompetent individuals, such as foci in Brazil where up to 17% of individuals suffer from ocular toxoplasmosis[3] and in French Guiana where severely lifethreatening manifestations of infection have been seen in immunocompetent patients.[4] A recent study suggests that a large fraction of individuals with ocular toxoplasmosis also have tachyzoites in the blood.[5] When initial infection with *T. gondii* occurs during pregnancy, it can be vertically transmitted, often leading to birth defects or miscarriage. A recent review of the literature illuminates the high prevalence of *T. gondii* infection in women of childbearing age.[6] Approximately 11% of the U.S. population is seropositive for *T. gondii*, with most studies of European populations reporting 20–35% seropositivity.[1, 7] In less developed countries, these rates can reach 50–75%.[6] Thus, many individuals who become immunocompromised are at risk for developing acute toxoplasmosis.

In immunocompetent individuals, toxoplasmosis is usually asymptomatic, but can appear as mild flu like symptoms in some instances. For these individuals, recovery usually occurs without anti-microbial treatment. However, the fact that toxoplasma infection is epidemiologically associated with schizophrenia suggests that some immunocompetent individuals may also suffer from other adverse health effects.[8] For immunocompromised individuals, intensive treatment is often required for the infection, with additional suppressive therapy necessary for the duration of the immunosuppression. This treatment can be for life in the case of patients with AIDS, though with immune reconstitution after highly active antiretroviral therapy, suppressive treatment can be stopped. Before the era of highly effective antiretrovirals, toxoplasmic encephalitis was the initial AIDS-defining illness in up to 33% of cases.[9] First line therapy for toxoplasmosis typically involves a combination regimen of pyrimethamine with a sulfa (sulfonamide) drug, such as sulfadiazine.[2] For patients with sensitivity to sulfa drugs, clindamycin can be administered in lieu of sulfadiazine. Leucovorin (folinic acid) is coadministered to mitigate the toxic effects that pyrimethamine has on bone marrow. Additionally, pyrimethamine is teratogenic and is thus contraindicated for use in women during their first trimester of pregnancy. While not as effective as pyrimethamine and sulfonamides, spiramycin is recommended in these circumstances and has proven moderately effective at reducing congenital transmission.[2, 10, 11] Unfortunately, spiramycin has yet to gain FDA approval in the United States. While other *T. gondii* anti-parasitic drugs are available, these agents also have significant drawbacks. Because of the toxicity associated with current toxoplasmosis therapeutics, complicated dosing regimens, and decreased effectiveness of second-line treatments when pyrimethamine and sulfonamides are contraindicated, there is the need to develop new *T. gondii* anti-parasitic drugs that are non-toxic to humans and possess simpler dosing profiles.

In developing new toxoplasmosis therapeutics, we are exploring enzyme targets that are involved in calcium-regulated biological processes, such as host cell invasion, gliding motility, and exocytosis.[12, 13] A key component of the signaling pathways that regulate these events is the calcium-dependent protein kinase, CDPK1. As calcium levels increase, CDPK1 is activated, leading to increased gliding and motility, which is important for both parasite invasion and egress.[14] Because *T. gondii* is an obligate intracellular parasite that requires invasion of mammalian host cells to proliferate, *Tg*CDPK1 represents a promising drug target for the development of anti-parasitic agents. We previously developed several ATP-competitive inhibitors of *Tg*CDPK1 enzymatic activity and confirmed that *Tg*CDPK1 inhibition prevents invasion of *T. gondii* into host cells, blocking parasite proliferation.[15, 16] A critical consideration of this anti-parasitic strategy is to minimize perturbation of off-target mammalian signaling pathways by selectively targeting *Tg*CDPK1 over the 518

kinases present in humans. We were able to accomplish this goal by exploiting a unique sequence and structural variation in the ATPbinding cleft of *Tg*CDPK1, where the presence of a small glycine gatekeeper residue permits large hydrophobic substituents displayed from the *C-3* position of the pyrazolopyrimidine scaffold to occupy an adjacent hydrophobic pocket (Figures 1 and 2). Human kinases contain gatekeeper residues with larger side chains that sterically occlude access to this pocket. Based on structure-activity relationships from our previous studies,[15, 16] we have developed an optimized panel of *Tg*CDPK1 inhibitors. Numerous compounds from this panel are extremely potent inhibitors of *Tg*CDPK1 activity *in vitro* and block *T. gondii* host cell invasion and proliferation. Several lead candidates were further shown to be highly selective for *Tg*CDPK1 over a panel of human kinases and additionally do not inhibit the growth of human cell lines, suggesting this anti-parasitic strategy could prove non-toxic to mammalian systems.

Results and Discussion

Molecular Design and Synthesis

We have previously shown that pyrazolopyrimidine-based molecules, variably substituted at the R_1 and R_2 positions of the core scaffold (Figure 1), are potent inhibitors of *Tg*CDPK1 enzymatic activity.[16] In that study, two distinct molecular series were developed to optimize compounds for inhibition of *Tg*CDPK1 enzymatic activity. The first series explored variation of the R_2 substructure in the context of a naphthylmethylene R_1-bearing pyrazolopyrimidine core scaffold (substituent **10** in Figure 1). From that series, several piperidine-containing R_2 substructures were found that confer potent inhibition of *Tg*CDPK1 enzymatic activity; the best being the 4-piperidinemethyl R_2 substructure of analogue **10n** (*Tg*CDPK1 IC_{50}=15 nM). X-ray crystallographic analysis showed that the 4-piperidinemethyl group orients towards the αD-helix and makes a solvent exposed salt bridge with the Glu135 side chain carboxylate (as exemplified in the co-crystal structure of compound **15n** bound to *Tg*CDPK1, presented in Figure 2B). The second series of inhibitors evaluated variation at the R_1 position and identified several groups that were superior to the naphthylmethylene substructure for conferring potent inhibition of *Tg*CDPK1 activity. These contain R_1 aryl groups directly linked to the pyrazolopyrimidine core (i.e., through a C_{aryl}-C_{aryl} linkage), which orients the R_1 substructures directly towards the Gly128 gatekeeper residue and into an adjacent hydrophobic pocket (Figure 2). This increases selectivity for *Tg*CDPK1 over potential off-target human kinases, which primarily contain threonine and larger gatekeeper residues that hinder access to this pocket.

Based on the structure-activity relationships generated in our previous study, we have designed, synthesized, and evaluated a subsequent panel of lead *Tg*CDPK1 enzyme inhibitors for their ability to prevent the invasion of *T. gondii* parasites into host cells. In the first part of this study, we have investigated a panel of R_1 groups in the context of ^{i}Pr-, ^{t}Bu-, and 4- piperidinemethyl-substituents at the R_2 position (series **a**, **b**, and **n** in Figure 1 and Table 1). To impart selective inhibition for *Tg*CDPK1 over human kinases, our efforts focused on R_1 substructures that occupy the enlarged hydrophobic pocket next to the Gly128 gatekeeper residue, such as substituted phenyls, indoles, indazoles, naphthyls, and quinolines (Figure 1). From previous structural studies,[15] it appeared that increased binding affinity could be gained by extending the R_1 substructure more deeply into the adjacent hydrophobic pocket (Figure 2C). To explore this possibility, analogues with extended R_1 groups (series **14**–**25**) were synthesized. Analysis of various R_2 substructures in the context of multiple R_1 groups allows the interdependence of these two positions to be explored.

Syntheses of pyrazolopyrimidine compounds with ^{i}Pr- or ^{t}Bu-groups at the R_2 position (series **a** and **b**) are outlined in Scheme 1. Detailed procedures and characterization data for all compounds are presented in the Supporting Information. Microwave-assisted Suzuki-

Miyaura reactions were employed for the coupling of R_1 boronic acids or boronate pinacol esters to the respective pyrazolopyrimidine halide intermediates **26** and **27**.[16, 17] For compounds **17a**–**25a**, containing extended R_1 substructures, Suzuki-Miyaura coupling of the TBDMS-protected boronic acid conveniently afforded the deprotected naphthol intermediate directly, which was subsequently alkylated with the respective R′-halide. Synthesis of the 4-piperidinemethyl-pyrazolopyrimidine compounds (series **n**) is outlined in Scheme 2. The pyrazolopyrimidine core scaffold intermediate **32** was synthesized according to previously reported procedures.[16, 17] Pyrazolopyrimidine **32** was then alkylated with mesylate **30** to afford the key intermediate **34**. Suzuki-Miyaura coupling of the respective R_1 boronic acids or boronate pinacol esters, and subsequent naphthol alkylations, were performed as described above for the series **a** and **b** compounds. Boc-containing compounds were deprotected using 50% TFA in CH_2Cl_2 and converted to their HCl salts for enzymatic and cell-based evaluation (results are discussed below and presented in Tables 1 and 2).

From the compounds described in Table 1, the 6-ethoxynaphthyl R_1 group (**15**) was identified as the best substructure for conferring potent inhibition of *Tg*CDPK1 enzymatic activity and *T. gondii* cell proliferation (*vide infra*). Therefore, a second series of compounds containing a 6-ethoxynaphthyl R_1 and variable R_2 substructures was generated (Figure 1 – substructures **a**-**w**). Syntheses of these compounds are presented in Scheme 3. For the piperidinyl-amide and sulfonamide compounds (**15l**, **15m**, **15q**, and **15r**), the pyrazolopyrimidine intermediate core **32** was alkylated with mesylates **36**, **37**, **40** and **41**, respectively, followed by microwave-assisted Suzuki-Miyaura coupling with 6-ethoxynaphthyl-2-boronic acid as described above (Scheme 3A). Compounds **15o** and **15p** were synthesized by reductive alkylation of **15n** with formaldehyde and acetaldehyde, respectively, using sodium cyanoborohydride (Scheme 3B). The remaining series **15** compounds were synthesized by first appending the 6- ethoxynaphthyl R_1 substructure to the pyrazolopyrimidine core scaffold **32** through microwaveassisted Suzuki-Miyaura couplings, affording intermediate **44**. Mitsunobu alkylation of the remaining R_2 groups using resin-bound PPh_3, followed by Boc-deprotection with TFA/CH_2Cl_2, afforded compounds **15c**, **15e**, **15g**, and **15s**. Reductive alkylation of the deprotected intermediates, with respective R_2-aldehydes, provided final compounds **15d**, **15f**, **15h-k**, and **15tw** (compounds **15k** and **15w** required additional Boc-deprotection). All compounds were purified by preparatory RP-HPLC and amine-containing compounds were converted to their HCl salts for enzymatic and cell-based evaluation (results are discussed below).

Pyrazolopyrimidines are potent inhibitors of *Tg*CDPK1 enzymatic activity

Compounds were first evaluated for their ability to inhibit the *in vitro* enzymatic activity of wild type *T. gondii* CDPK1. Inhibition was determined using a previously reported luminescence-based kinase assay.[16] Although a large percentage of the compounds tested displayed very potent inhibition of *Tg*CDPK1, several notable trends were observed. While the absence of a hydrophobic substituent at the R_1 position renders these pyrazolopyrimidine compounds inactive against *Tg*CDPK1 (the IC_{50} values for **1b** and **1n** are >5 μM, Table 1), incorporation of R_1 substructures as small as a phenyl group confers potent enzymatic inhibition. Overall, 86% of the compounds tested have IC_{50} values <25 nM against *Tg*CDPK1 (Table 1). When compared with results obtained in our previous study,[16] it is evident that coupling of an R_1 substructure to the pyrazolopyrimidine core through a direct C_{aryl}-C_{aryl} linkage provides analogues with superior potency relative to those that contain a methylene spacer (for example, series **10**). As observed from crystallographic studies, this direct linkage orients the R_1 substructures towards the adjacent pocket next to the Gly128 gatekeeper residue, allowing large hydrophobic groups to make extensive contacts (Figure 2).[18] In the context of the 6- ethoxynaphthyl R_1 substructure (series **15**), it appears that a wide variety of substitutions at the R_2 position are well tolerated for maintaining potent

*Tg*CDPK1 enzymatic inhibition (Table 3), which is in contrast to analogues that contain a napthylmethylene group at this position. For example, series **15** compounds (6-ethoxynaphthyl R_1) that are alkylated, acetylated, or sulfonylated on the piperidine rings of their R_2 substructures maintain low nanomolar inhibition of *Tg*CDPK1 enzymatic activity, whereas series **10** analogues (naphthylmethylene R_1) containing similar modifications demonstrate IC_{50} values in the high nanomolar range. Consistently potent inhibition across a wide range of R_1 and R_2 substructures suggests there is ample chemical space at either position to exploit for optimizing the pharmacological properties of these inhibitors.

To determine how a larger gatekeeper residue affects compound binding, inhibitors were tested against a *Tg*CDPK1 mutant enzyme that contains methionine at this position (Gly128Met). Molecular modeling predicts that the increased steric bulk of this residue should clash with large R_1 substructures (Figure 2B). In addition, the Gly128Met mutant was selected as a drug-resistant mutant because it maintains comparable enzymatic activity to wild type *Tg*CDPK1 and is able to complement for loss of endogenous enzyme activity in *T. gondii* parasites. In nearly all cases, the presence of the larger methionine side chain abolishes the inhibitory activity of these molecules (IC_{50} values are generally >3 μM). Even for compounds **22n**, **24n**, **25n**, **15h**, **15k**, and **15s-w**, which show some activity against Gly128Met *Tg*CDPK1, the differences in IC_{50} values between the wild type and mutant enzymes are >250-fold (with the exception of **15w**, which displays a 68-fold difference). Thus, the presence of a small gatekeeper residue provides a distinct preference for binding to the wild type enzyme. These results are promising for the development of pyrazolopyrimidine inhibitors as potential anti-parasitic drugs because it suggests we should be able to obtain selectivity for *Tg*CDPK1 over human kinases, which do not contain gatekeeper residues as small as Gly or Ala.

Lead compounds selectively inhibit *Tg*CDPK1 over human kinases and do not inhibit growth of human cell lines

While compound evaluation in the Gly128Met *Tg*CDPK1 enzymatic assay was an important surrogate for gauging potential inhibition of off-target kinases that contain larger gatekeeper residues in an otherwise identical binding site, further evaluation was performed against a panel of human kinases. Compounds were first tested against SRC kinase, as prior selectivity studies have demonstrated that similar pyrazolopyrimidine-based inhibitors preferentially target this enzyme.[19–21] Since SRC contains a threonine gatekeeper residue, which is one of the smallest amino acid side chains present at this position in human kinases, we selected this enzyme as a surrogate for probing potential off-target kinase activity. Inhibition of this enzyme serves as a first-pass filter to prioritize lead candidates for subsequent cell-based evaluation. Inhibition values were determined using a previously reported radioactive kinase assay.[16]

The activities of the first series of compounds against SRC are shown in Table 1. While we had initially envisioned the R_1 substructure providing the primary determinant for obtaining selective inhibition of *Tg*CDPK1 over human kinases (i.e., a steric clash of the R_1 substructures with the larger gatekeeper residue side chains obstructs ligand binding), this appears to be only partially true. For 93% of the compounds tested, IC_{50} values are at least 25-fold higher for SRC than for *Tg*CDPK1 (Table 1). Thus, substitution at the R_1 substructure is a significant determinant of selective inhibition of *Tg*CDPK1. However, further examination of the results presented in Table 1, where we have evaluated R_1 substructures in the context of ^{i}Pr (**a**), ^{t}Bu (**b**), and 4-piperidinemethyl (**n**) R_2 substituents, demonstrates a striking trend where the ^{i}Pr- and ^{t}Bucontaining compounds are consistently less selective for *Tg*CDPK1 over SRC than the 4- piperidinemethyl analogues (differences are readily observed in the inhibition heat maps in Tables 2A and B, and Figure S1 in the Supporting Information). The second compound series, where we have evaluated R_2

substructures in the context of a 6-ethoxynapthyl (**15**) group at the R_1 position, was tested against SRC to further probe this interesting phenomenon (Table 3). In this series, it appears that compounds which contain a methylene spacer adjacent to the pyrazolopyrimidine core display greater selectivity for *Tg*CDPK1 inhibition over SRC. 4- piperidinemethyl-containing compounds (**n-r**) are particularly selective and display no inhibition of SRC activity at compound concentrations upwards of 10 μM. Thus, it is evident that the degree of selective inhibition of *Tg*CDPK1 over SRC results from a synergy between the R_1 and R_2 substructures. A more detailed discussion of the structural underpinnings for this synergy will be presented in a forthcoming X-ray crystallography manuscript.[18]

Several lead compounds (**14a**, **14n**, **15a**, **15h**, **15n**, **15o**, and **16n**) were further evaluated in an expanded panel of human kinases that all contain threonine gatekeeper residues (ABL, LCK, p38α, EPHA3, CSK, and EGFR). In general, similar inhibition trends were observed for ABL, p38α, EPHA3, CSK, and EGFR as described above (Table 4). In comparison to SRC, compounds generally display increased inhibition of LCK, equipotency against ABL and EGFR, and decreased inhibition of p38α, EPHA3, and CSK, which is similar to trends that have been previously reported.[19] Importantly, we generally observe >1000-fold differences between IC_{50} values for *Tg*CDPK1 over human kinases for our lead inhibitors (**14n**, **15h**, **15n**, **15o**, and **16n;** refer to Table S1 in the Supporting Information for specific selectivity ratios between the human kinase IC_{50} values compared to *Tg*CDPK1). While these compounds have only been tested against a small panel of enzymes that were envisioned to be of primary concern for inhibition, these results suggest our lead candidate *T. gondii* therapeutics should interact minimally with potential off-target human kinases.

As an indicator for potential host cell toxicity during toxoplasmosis therapy, we further evaluated our panel of *Tg*CDPK1 inhibitors (**14a**, **14n**, **15a**, **15h**, **15n. 15o**, and **16n**) for their ability to inhibit the growth of human neutrophil (HL-60) and lymphocyte (CRL-8155) cell lines. Assays were performed with a similar procedure as previously reported.[16] These compounds exhibited no inhibition of cell growth at concentrations up to 10 μM (Table 4). To better define potential therapeutic windows for our toxoplasmosis drug candidates, we are performing growth inhibition studies using higher compound concentrations and identifying drug levels required to clear parasitic infection in mammalian challenge models. Results from these studies will be presented elsewhere.

Potent *Tg*CDPK1 enzymatic inhibitors block the proliferation of *T. gondii* parasites

Having developed compounds that selectively inhibit *Tg*CDPK1 over a panel of human kinases and do not inhibit the growth of human cell lines, we further investigated the most potent *Tg*CDPK1 enzymatic inhibitors (IC_{50} < 25 nM) for their efficacy in blocking the invasion of *T. gondii* parasites into human foreskin fibroblast cells. Since *T. gondii* is an obligate intracellular parasite, inhibition of host cell invasion blocks parasite replication, which was measured as a surrogate according to a slightly modified version of a previously reported procedure.[15] In these cellular assays, several prominent trends were observed. Notably, compounds **1b** and **1n**, which do not contain an R_1 substituent and are inactive against *Tg*CDPK1 enzymatic activity, do not block *T. gondii* cell invasion/proliferation. Of the compounds that do potently inhibit *Tg*CDPK1 enzymatic activity (IC_{50} < 25 nM), an impressive 84% also effectively block *T. gondii* cell invasion/proliferation (EC_{50} < 1 μM). Importantly, no inhibitor toxicity was observed against the human foreskin fibroblasts used in this assay. Thus, it seems unlikely that the decreased parasite growth is an artifact of host cell inhibition. Many of the 4-piperidinemethyl compounds are potent inhibitors of *T. gondii* proliferation. In particular, compounds bearing the 6- ethoxynaphthyl R_1 substructure (series **15**) are potent enzymatic and cell proliferation inhibitors across nearly the entire R_2 substructure panel. However, compounds containing an ^{i}Pr or ^{t}Bu group at the R_2 position (series **a** and **b**, respectively) are generally more potent inhibitors in the cell proliferation

assay than their 4-piperidinemethyl analogues (series **n**). This is readily observed in Figure 3A and in the inhibition heat map presented in Table 2C. The **a** and **b** series of inhibitors are significantly more hydrophobic than the 4-piperidinemethyl-containing compounds (the piperidine amine would be protonated under physiological conditions), which may increase their membrane permeability. In addition, the greater potential of pyrazolopyrimidine inhibitors with ^{i}Pr and ^{t}Bu substituents at the R_2 position to inhibit off-target mammalian and parasitic kinases (as suggested by their more potent inhibition of SRC and other human kinases), may lead to enhanced cellular activity. While it is interesting to speculate on the biophysical underpinnings of these differences, SAR rationalizations in these cellular assays are likely to be complicated and beyond the scope of this manuscript.

Three compounds (**15n**, **15o**, and **16n**) were evaluated in cell-based experiments using *T. gondii* parasites expressing the Gly128Met *Tg*CDPK1 gatekeeper mutant, to further validate that *Tg*CDPK1 is the primary target for the observed anti-parasitic activity. The Gly128Met *Tg*CDPK1 variant is functionally active and complements the loss of endogenous wild type enzyme activity, permitting parasite invasion and proliferation in host cells. For all three compounds, a significant increase in *T. gondii* proliferation EC_{50} (8- to 26-fold) was observed for parasites expressing the Gly128Met *Tg*CDPK1 mutant over those expressing wild type *Tg*CDPK1 at similar levels or non-transfected parasites (Figure 3B and Figures S3A and S3B in the Supporting Information). The observed inhibitory effects at higher compound concentrations (EC_{50} ~1 to 3 μM for the Gly128Met *Tg*CDPK1 expressing parasites) could indicate off-target inhibition of another parasite kinase. However, the dramatic EC_{50} shifts seen for all three inhibitors demonstrate that *Tg*CDPK1 is the primary target for blocking parasite invasion and proliferation.

Conclusions

In the present study, we have evaluated over 70 ATP-competitive inhibitors of *Tg*CDPK1 for their utility as potential toxoplasmosis therapeutics. We found that inhibition of *Tg*CDPK1 enzymatic activity correlates strongly with inhibition of *T. gondii* proliferation. Of the 64 compounds that are potent inhibitors of *Tg*CDPK1 enzymatic activity *in vitro* (IC_{50} < 25 nM), 83% exhibit EC_{50} values of <1 μM in a parasite invasion/proliferation assay. Furthermore, 38% exhibit EC_{50} values <100 nM. In a rescue experiment, expression of the drug-resistant Gly128Met *Tg*CDPK1 enzyme in parasites verified that inhibition of endogenous wild type CDPK1 is the primary mechanism of action for these compounds. By virtue of the small glycine gatekeeper residue in wild type *Tg*CDPK1, these “bumped” kinase inhibitors are able to selectively inhibit the parasite enzyme over human kinases, which contain gatekeeper residues larger than glycine that sterically hinder inhibitor binding. This selectivity is mimicked in cellular assays where compounds potently inhibit *T. gondii* proliferation, but do not affect the growth of human cell lines. Compounds exhibiting large therapeutic windows between inhibition of *T. gondii* proliferation and human cell growth (e.g. >100–1000x) are undergoing additional pre-clinical drug development testing to evaluate pharmacological properties such as solubility, pharmacokinetics, pharmacodynamics, and metabolism. The results obtained here poise us for future studies to evaluate lead candidates possessing favorable properties in parasitic challenge models in mice as a therapeutic proof of principle.

Experimental Procedures

General synthetic methods

Unless otherwise stated, all chemicals were purchased from commercial suppliers and used without further purification. Reaction progress was monitored by thin-layer chromatography on silica gel 60 F254 coated glass plates (EM Sciences). Chromatography was performed

using an IntelliFlash 280 automated flash chromatography system, eluting on prepacked Varian SuperFlash silica gel columns with hexanes/EtOAc or CH_2Cl_2/MeOH gradient solvent systems. For preparatory HPLC purification, samples were chromatographically separated using a Varian Dynamax Microsorb 100-5 C_{18} column (250 mm × 21.4 mm), eluting with H_2O/CH_3CN or H_2O/MeOH gradient solvent systems (+0.05% TFA). The purity of all final compounds was determined by two analytical RP-HPLC methods, using an Agilent ZORBAX SB-C_{18} (2.1 mm × 150 mm) or Varian Microsorb-MV 100-5 C_{18} column (4.6 mm × 150 mm), and eluting with either H_2O/CH_3CN or H_2O/MeOH gradient solvent systems (+0.05% TFA) run over 30 min. Products were detected by UV at λ=254 nm, with all final compounds displaying >95% purity. NMR spectra were recorded on Bruker 300 or 500 MHz spectrometers at ambient temperature. Chemical shifts are reported in parts per million (δ) and coupling constants in Hz. ^{1}H-NMR spectra were referenced to the residual solvent peaks as internal standards (7.26 ppm for $CDCl_3$, 2.50 ppm for d_6-DMSO, and 3.34 ppm for CD_3OD). Mass spectra were recorded with a Bruker Esquire Liquid Chromatograph - Ion Trap Mass Spectrometer. Inhibitors were synthesized through several different routes, as represented in Schemes 1–3. Syntheses of compounds **1b**, **3a**, **4a**, **5a**, **10a**, **10b**, **10n**, **11a**, **11b**, **12a**, **14a**, **15a**, **26**, **27**, **31**, and **32** have been previously reported.[16, 17] All other synthesis and compound characterization data is presented in the Supporting Information.

T. gondii CDPK1 enzymatic assays

Expression, purification, and enzymatic evaluation of wild type and Gly128Met gatekeeper mutant *Tg*CDPK1 was performed as described previously.[15, 16] Briefly, enzymatic reactions were performed with 4 nM of either wild type or Gly128Met *Tg*CDPK1 in assay buffer containing 20 mM HEPES (pH=7.5), 0.1% BSA, 10 mM $MgCl_2$, 1 mM EGTA, 2 mM $CaCl_2$, 10 μM ATP, and 40 μM Syntide-2 peptide substrate (peptide sequence: PLARTLSVAGLPGKKOH). After incubating for 90 min at 30 °C, the enzymatic reactions were terminated by adding EGTA to a final concentration of 5 mM. The amount of ATP remaining in solution was evaluated using the Kinase Glo luciferase assay from Promega, with sample luminescence read using a Microbeta 2 plate reader (Perkin Elmer, Waltham, MA). Results were converted to percent inhibition and IC_{50} values were calculated using non-linear regression analysis in GraphPad Prism. Compounds were evaluated in triplicate in 8 point dilutions (3-fold dilution series) during the enzymatic reactions.

Human kinase enzymatic assays

All compounds were evaluated in a primary counter-screen against SRC kinase using either the truncated catalytic kinase domain (SRCKD) or the full length three domain enzyme (SRC3D). Results from compounds tested with both KD and 3D enzymes demonstrated no significant difference in IC_{50} values, and are thus reported together simply as inhibition of "SRC" kinase. Lead compounds were further evaluated against a small panel of additional human kinases – ABL, LCK, p38α, EPHA3, CSK, and EGFR. Compounds were evaluated in 10 point, 3-fold dilution series ranging from 10 μM to 0.5 nM during the enzymatic reactions, as per previously reported procedures.[16] Results were converted to percent inhibition and IC_{50} values were calculated using non-linear regression analysis in GraphPad Prism. Experiments were performed in triplicate or quadruplicate. Assay buffers, enzyme concentrations, substrate peptide sequences and concentrations, and enzymatic reaction times are listed in the assay-specific details presented below. All assays were performed using <5 μM ATP ([ATP] ≪ K_m).

1. SRC – Kinase concentration during the enzymatic reaction: 1 nM for SRCKD or 2 nM for SRC3D. Assay buffer: 33.5 mM HEPES, pH=7.5, 6.7 mM $MgCl_2$, 1.7 mM EGTA, 67 mM NaCl, 2 mM Na_3VO_4, 0.08 mg/ml BSA, γ^{32}P ATP (0.2 μCi/well).

Enzymatic reaction time: 30 min for SRCKD or 60 min for SRC3D. Substrate peptide sequence and concentration: Ac- EIYGEFKKK-OH (100 μM).

2. ABL – Kinase concentration during the enzymatic reaction: 1 nM for ABLKD or 2 nM for ABL3D. Assay buffer: 33.5 mM HEPES, pH=7.5, 6.7 mM $MgCl_2$, 1.7 mM EGTA, 67 mM NaCl, 2 mM Na_3VO_4, 0.08 mg/ml BSA, γ^{32}P ATP (0.2 μCi/well). Enzymatic reaction time: 30 min for ABLKD and 60 min for ABL3D. Substrate peptide sequence and concentration: Ac-EAIYAAPFAKKK-OH (100 μM).
3. LCK – Kinase concentration during the enzymatic reaction: 10 nM. Assay buffer: 75 mM HEPES, pH=7.5, 15 mM $MgCl_2$, 3.75 mM EGTA, 150 mM NaCl, 2 mM Na_3VO_4, 0.08 mg/mL BSA, γ^{32}P ATP (0.2 μCi/well). Enzymatic reaction time: 60 min. Substrate peptide sequence and concentration: Ac-EIYGEFKKK-OH (100 μM).
4. p38α – Kinase concentration during the enzymatic reaction: 2 nM. Assay buffer: 75 mM HEPES, pH=7.5, 15 mM $MgCl_2$, 3.75 mM EGTA, 150 mM NaCl, 2 mM Na_3VO_4, 0.08 mg/mL BSA, 1.9 mM BME, γ^{32}P ATP (0.2 μCi/well). Enzymatic reaction time: 180 min. Substrate peptide and concentration: Myelin Basic Protein (0.2 mg/mL).
5. EPHA3 – Kinase concentration during the enzymatic reaction: 10 nM. Assay buffer: 30 mM HEPES, pH=7.5, 38 mM $MgCl_2$, 630 μM EGTA, 2 mM Na_3VO_4, 40 μg/ml BSA, γ^{32}P ATP (0.2 μCi/well). Enzymatic reaction time: 120 min. Substrate peptide and concentration: Myelin Basic Protein (0.2 mg/mL).
6. CSK – Kinase concentration during the enzymatic reaction: 5 nM. Assay buffer: 75 mM HEPES, pH=7.5, 15 mM $MgCl_2$, 3.75 mM EGTA, 150 mM NaCl, 2 mM Na_3VO_4, 0.2 mg/mL BSA, γ^{32}P ATP (0.2 μCi/well). Enzymatic reaction time: 180 min. Substrate peptide sequence and concentration: Ac-KKKKEEIYFFF-OH (130 μM).
7. EGFR – Kinase concentration during the enzymatic reaction: 1 nM. Assay buffer: 37.5 mM Tris, pH=7.5, 15 mM $MgCl_2$, 0.75 mM EGTA, 0.75 mM Na_3VO_4, 0.015% Triton X-100, 3.75 mM DTT, 0.08 mg/mL BSA, 2 mM ATP, γ^{32}P ATP (2.0 μCi/well). Enzymatic reaction time: 30 min. Substrate peptide and concentration: Poly Glu-Tyr substrate (0.2 mg/mL).

Human cell growth inhibition assays

Lead compounds were evaluated for potential toxicity against two human cell lines: HL- 60 (neutrophil) and CRL-8155 (lymphocytic) cells. Cells were grown in either IMDM (HL-60) or RPMI-1640 (CRL-8155) growth media supplemented with 10% heat inactivated fetal calf serum and 2 mM L-glutamine. HL-60 growth medium additionally contained 25 mM HEPES and 1% penicillin/streptomycin. CRL-8155 growth medium additionally contained 10 mM HEPES, 1 mM sodium pyruvate, 4.5 g/L glucose and 1.5 g/L sodium bicarbonate. Cells were grown in the presence of 10 μM test compound for 48 or 72 hours at 37°C and 5% CO_2 in 96- well flat-bottom plates (Corning). Growth was quantified using Alamar Blue as a developing reagent and detecting sample absorbance at λ = 570 nm (600 nm reference wavelength). Percent growth inhibition by test compounds were calculated based on cultures incubated with DMSO negative and tipifarnib (R115777) positive controls (0% and 100% growth inhibition, respectively). All assays were performed in triplicate.

T. gondii cell proliferation assays

The invasion assay was performed as previously described,[15] with slight modifications to improve assay sensitivity and reliability. Compounds were diluted in DMEM maintaining

0.5% DMSO. *T. gondii* clonal parasites (10^3) expressing β-galactosidase as a reporter (genotype RH*Δhxgprt*, β-galactosidase, GFP[15] for the standard protocol) were mixed with the medium containing the compounds (200 μl) and incubated at 37°C, 5% CO_2, for ~5min. The parasite/compound mixture was added to 96-well plates containing confluent human fibroblast cell layers (from which growth media was aspirated) and incubated for 44 hours at 37°C and 5% CO_2. As a control, a dilution series of *T. gondii* (10^3-0) parasites was grown in the same conditions described above, but without compound. Plates were visually inspected for evidence of cytotoxic effects on fibroblasts. β-galactosidase was then assayed using chlorophenol red β-galactopyranose (Sigma) as a substrate.[22] Plates were developed for ~1.5 hours at 37°C. Absorbance was measured at 595 nm on a SpectraMax M2 (Molecular Devices) microplate reader. Each experiment was performed in triplicate and experiments yielding EC_{50} values < 0.5 μM were repeated at least once. For assays to test the role of the gatekeeper residue, the above procedure was followed except that three *T. gondii* cell lines expressing β-galactosidase in either a "wild type" background (as above in the standard assay) or also expressing HA-*Tg*CDPK1 or HA-Gly128Met *Tg*CDPK1 or were assayed in parallel.

Supplementary Material

Refer to Web version on PubMed Central for supplementary material.

Acknowledgments

We are grateful for the technical assistance of Suzanne Scheele from the Parsons lab. This work was funded by the National Institute of General Medical Sciences Grant R01GM086858 (D.J.M.) and the National Institute of Allergy and Infectious Diseases Grants R01AI080625 (W.C.V.V.) and R01AI067921 (E.A.M. and W.C.V.V.). J.A.G. was supported by a training grant from the National Institute of Allergy and Infectious Diseases T32AI007509.

Abbreviations List

ATP	adenosine triphosphate
Boc	*tert*-butyloxycarbonyl
CDPK1	calciumdependent protein kinase 1
CSK	*C*-terminal SRC kinase
DIAD	diisopropyl azodicarboxylate
DME	dimethoxyethane
EC_{50}	half maximal effective concentration
EGFR	epidermal growth factor receptor kinase
EPHA3	EPH receptor A3 kinase
IC_{50}	half maximal inhibitory concentration
LCK	lymphocyte-specific protein tyrosine kinase
TBDMS	*t*-butyldimethylsilyl

References

1. Tenter AM, Heckeroth AR, Weiss LM. Toxoplasma gondii: from animals to humans. Int J Parasitol. 2000; 30:1217–1258. [PubMed: 11113252]
2. Schwartzman, JD.; Maguire, JH. Tropical Infectious Diseases: Principles, Pathogens and Practice. 3. W.B. Saunders; Edinburgh: 2011. CHAPTER 103 - Toxoplasmosis; p. 722-728.

3. Jones JL, Muccioli C, Belfort R Jr, Holland GN, Roberts JM, Silveira C. Recently acquired Toxoplasma gondii infection Brazil. Emerg Infect Dis. 2006; 12:582–587. [PubMed: 16704805]
4. Demar M, Hommel D, Djossou F, Peneau C, Boukhari R, Louvel D, Bourbigot AM, Nasser V, Ajzenberg D, Darde ML, Carme B. Acute toxoplasmoses in immunocompetent patients hospitalized in an intensive care unit in French Guiana. Clin Microbiol Infect. [Online early access]. Published Online: September 29, 2011. 10.1111/j.1469–0691.2011.03648.x
5. Silveira C, Vallochi AL, Rodrigues da Silva U, Muccioli C, Holland GN, Nussenblatt RB, Belfort R, Rizzo LV. Toxoplasma gondii in the peripheral blood of patients with acute and chronic toxoplasmosis. Br J Ophthalmol. 2011; 95:396–400. [PubMed: 20601663]
6. Pappas G, Roussos N, Falagas ME. Toxoplasmosis snapshots: global status of Toxoplasma gondii seroprevalence and implications for pregnancy and congenital toxoplasmosis. Int J Parasitol. 2009; 39:1385–1394. [PubMed: 19433092]
7. Jones JL, Kruszon-Moran D, Sanders-Lewis K, Wilson M. Toxoplasma gondii infection in the United States, 1999–2004, decline from the prior decade. Am J Trop Med Hyg. 2007; 77:405–410. [PubMed: 17827351]
8. Yolken RH, Torrey EF. Are some cases of psychosis caused by microbial agents? A review of the evidence. Mol Psychiatry. 2008; 13:470–479. [PubMed: 18268502]
9. Dubey JP, Jones JL. Toxoplasma gondii infection in humans and animals in the United States. Int J Parasitol. 2008; 38:1257–1278. [PubMed: 18508057]
10. Montoya JG, Liesenfeld O. Toxoplasmosis. Lancet. 2004; 363:1965–76. [PubMed: 15194258]
11. Montoya JG, Remington JS. Management of Toxoplasma gondii infection during pregnancy. Clin Infect Dis. 2008; 47:554–566. [PubMed: 18624630]
12. Nagamune K, Sibley LD. Comparative genomic and phylogenetic analyses of calcium ATPases and calcium-regulated proteins in the apicomplexa. Mol Biol Evol. 2006; 23:1613– 1627. [PubMed: 16751258]
13. Lourido S, Shuman J, Zhang C, Shokat KM, Hui R, Sibley LD. Calciumdependent protein kinase 1 is an essential regulator of exocytosis in Toxoplasma. Nature. 2010; 465:359–362. [PubMed: 20485436]
14. Kieschnick H, Wakefield T, Narducci CA, Beckers C. Toxoplasma gondii attachment to host cells is regulated by a calmodulin-like domain protein kinase. J Biol Chem. 2001; 276:12369–12377. [PubMed: 11154702]
15. Ojo KK, Larson ET, Keyloun KR, Castaneda LJ, Derocher AE, Inampudi KK, Kim JE, Arakaki TL, Murphy RC, Zhang L, Napuli AJ, Maly DJ, Verlinde CL, Buckner FS, Parsons M, Hol WG, Merritt EA, Van Voorhis WC. Toxoplasma gondii calcium-dependent protein kinase 1 is a target for selective kinase inhibitors. Nat Struct Mol Biol. 2010; 17:602–607. [PubMed: 20436472]
16. Murphy RC, Ojo KK, Larson ET, Castellanos-Gonzalez A, Perera BG, Keyloun KR, Kim JE, Bhandari JG, Muller NR, Verlinde CL, White AC Jr, Merritt EA, Van Voorhis WC, Maly DJ. Discovery of Potent and Selective Inhibitors of Calcium-Dependent Protein Kinase 1 (CDPK1) from C. parvum and T. gondii. ACS Med Chem Lett. 2010; 1:331–335. [PubMed: 21116453]
17. Bulawa, CE.; Devit, M.; Elbaum, D. Preparation of pyrazolopyrimidinamines as modulators of protein trafficking. WO. 2009062118A2. 2009.
18. Larson ET, Ojo KK, Murphy RC, Johnson SM, Zhang Z, Kim JE, Leibly DJ, Fox AMW, Reid MC, Dale EJ, Perera BGK, Kim J, Hewitt SN, Hol WGJ, Verlinde CLMJ, Fan E, Van Voorhis WC, Maly DJ, Merritt EA. Unpublished results.
19. Bain J, Plater L, Elliott M, Shpiro N, Hastie CJ, McLauchlan H, Klevernic I, Arthur JS, Alessi DR, Cohen P. The selectivity of protein kinase inhibitors: a further update. Biochem J. 2007; 408:297–315. [PubMed: 17850214]
20. Hanke JH, Gardner JP, Dow RL, Changelian PS, Brissette WH, Weringer EJ, Pollok BA, Connelly PA. Discovery of a novel, potent, and Src family-selective tyrosine kinase inhibitor. Study of Lck- and FynT-dependent T cell activation. J Biol Chem. 1996; 271:695–701. [PubMed: 8557675]
21. Liu Y, Bishop A, Witucki L, Kraybill B, Shimizu E, Tsien J, Ubersax J, Blethrow J, Morgan DO, Shokat KM. Structural basis for selective inhibition of Src family kinases by PP1. Chem Biol. 1999; 6:671–678. [PubMed: 10467133]

22. Seeber F, Boothroyd JC. Escherichia coli beta-galactosidase as an in vitro and in vivo reporter enzyme and stable transfection marker in the intracellular protozoan parasite Toxoplasma gondii. Gene. 1996; 169:39–45. [PubMed: 8635747]

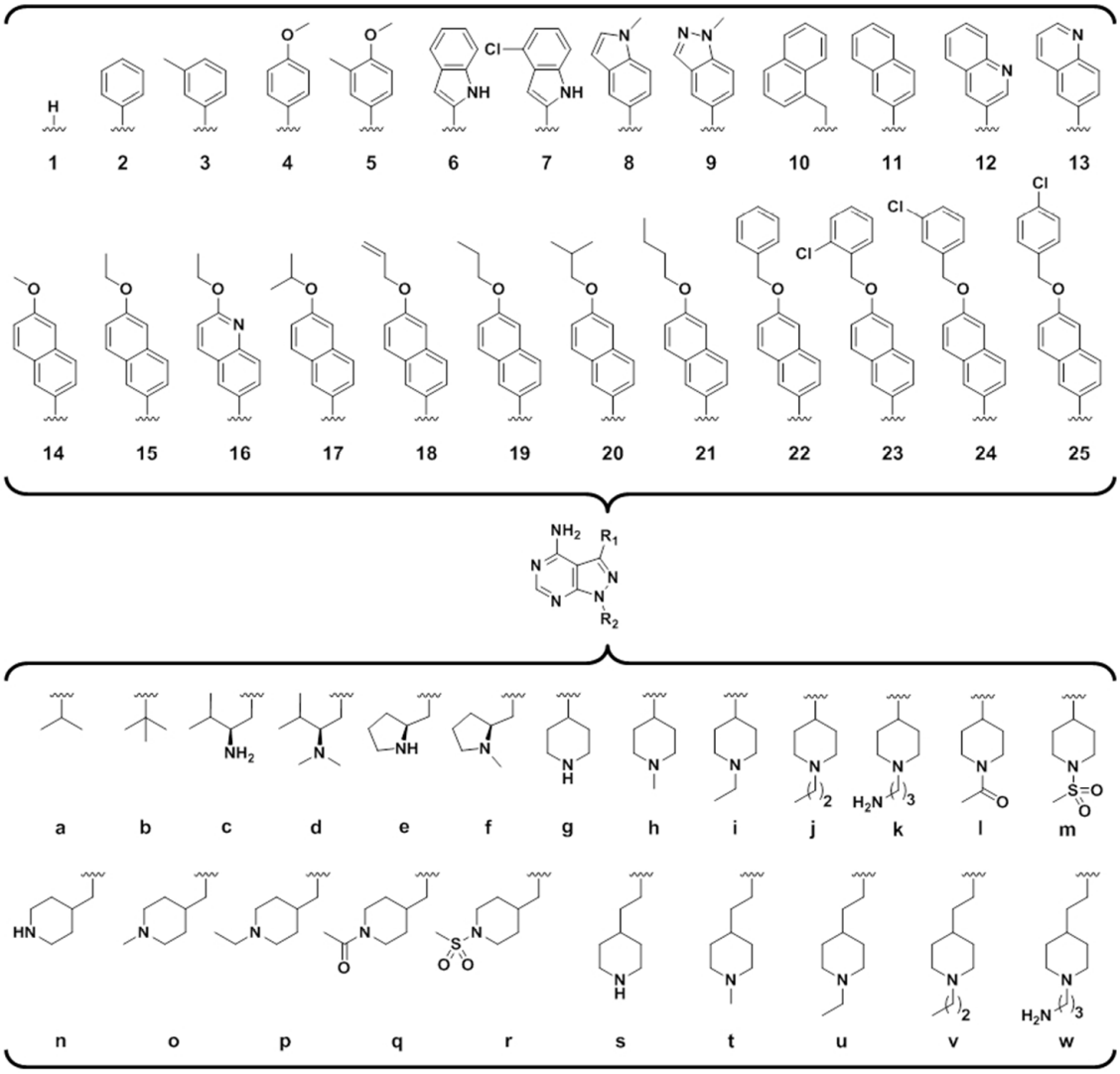

Figure 1.
Legend of the R_1 and R_2 substructures of compounds evaluated in this study.

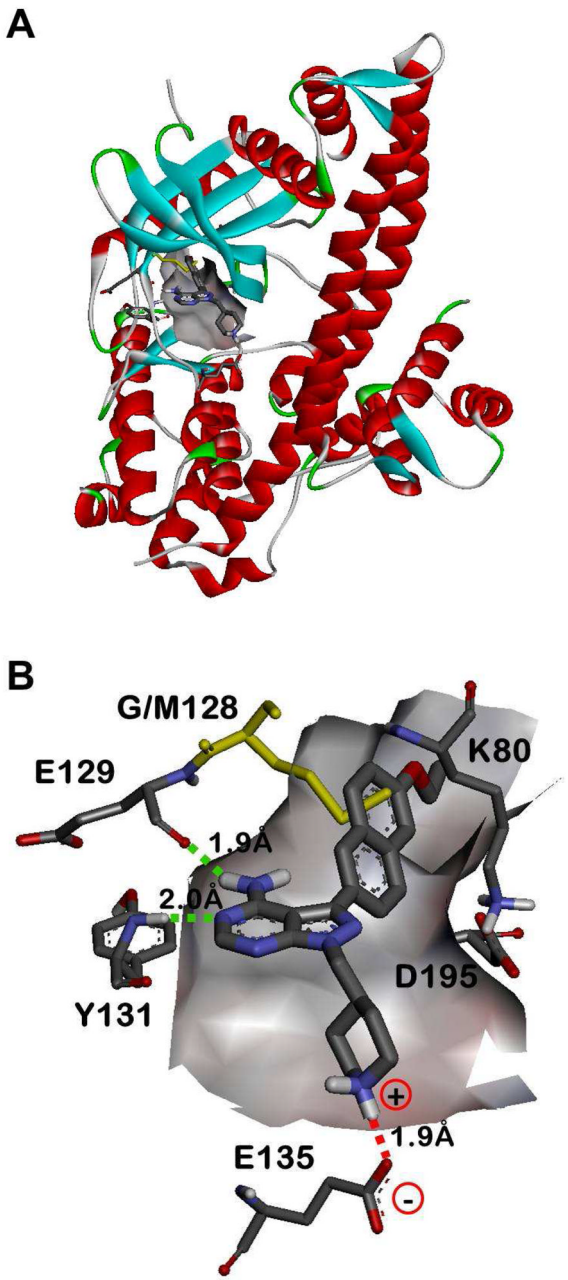

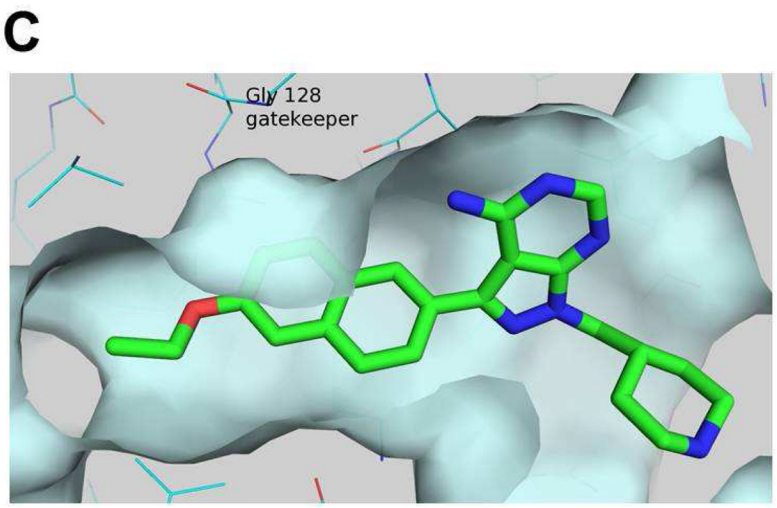

Figure 2.

X-ray crystallographic structure of compound **15n** bound to wild type *T. gondii* CDPK1 (PDB accession code: 3SX9).[18] A) Complete view of the **15n**•*Tg*CDPK1 co-crystal structure. B) Expanded view of the ATP binding site from panel A (protein backbone ribbons have been removed for clarity). The backbone carbonyl of Glu129 and NH of Tyr131 hydrogen bond with the exocyclic amine and adjacent endocyclic nitrogen of the pyrazolopyrimidine core, respectively (green dashed lines). The Glu135 side chain carboxylate makes a solvent exposed salt bridge with the piperidine R_2 ring, which is protonated under physiological conditions (red dashed line). The R_1 aryl substructure orients towards the Gly128 gatekeeper residue and into the adjacent hydrophobic pocket. The mutant Met128 residue (yellow) has been overlayed to show the steric clash that would occur between a larger gatekeeper side chain with the inhibitor R_1 substructures. The catalytic Lys80 and Asp195 side chains are also shown for context. C) Rotated, side/bottom view of the ATP binding site from panel B.

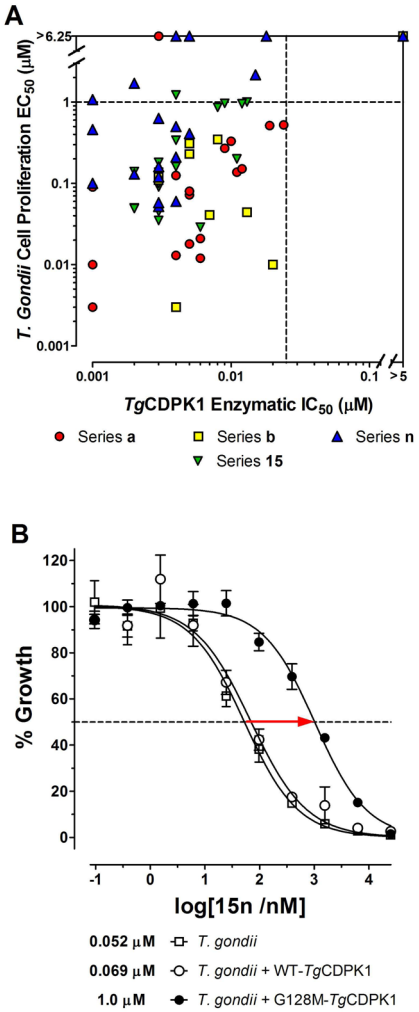

Figure 3.

Enzymatic and cellular inhibition of *Tg*CDPK1. A) Correlation between *T. gondii* cell proliferation EC_{50} and *Tg*CDPK1 enzymatic IC_{50} results. The solid lines at EC_{50} >6.25 μM and IC_{50} >5 μM represent the upper detection limits for compounds tested in the respective assays. Of the 62 compounds displaying a *Tg*CDPK1 enzymatic IC_{50} <0.025 μM, 86% are also potent inhibitors of *T. gondii* invasion/proliferation (EC_{50} <1 μM, points in bottom left quadrant). B) Comparison of EC_{50} curves between wild type *T. gondii* (open squares) and parasites expressing either wild type *Tg*CDPK1 (open circles) or the drug resistant Gly128Met *Tg*CDPK1 mutant (closed circles). Expression of the drug resistant Gly128Met *Tg*CDPK1 mutant rescues cells from the potent anti-proliferative effects of inhibitor **15n**.

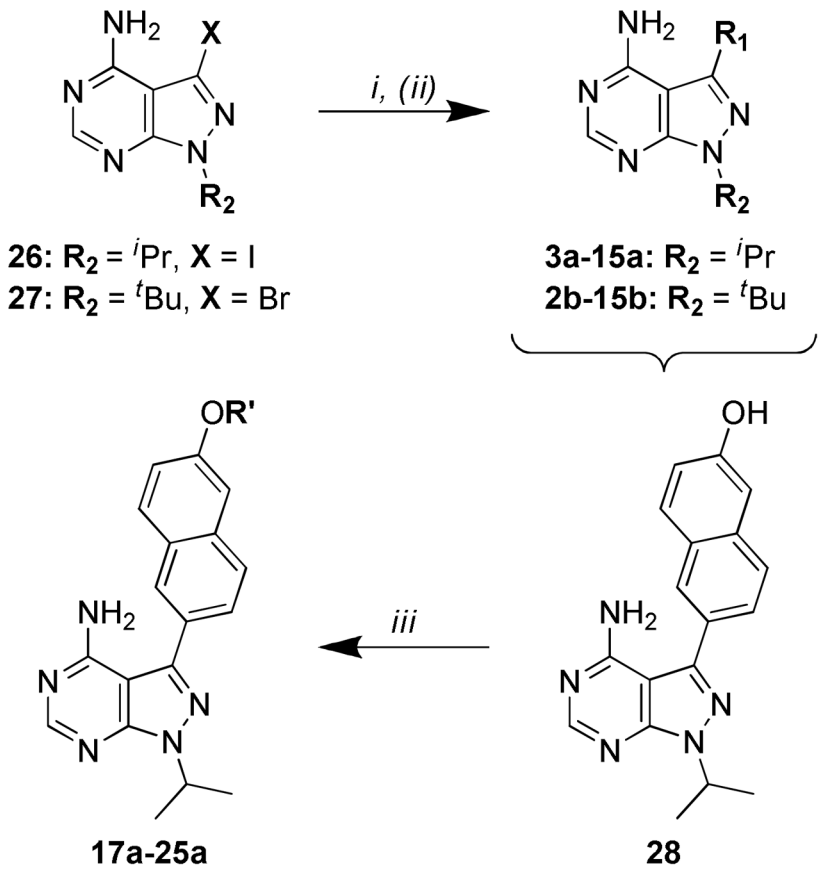

Scheme 1.

General synthetic procedures for compound series **a** and **b**. *i*) Na_2CO_3, $Pd(PPh_3)_4$, boronic acid or boronate pinacol ester, H_2O/DME, 80°C; *ii*) TFA/CH_2Cl_2 (for Boc-protected R_1 substructures **6** and **7**); *iii*) R′-halide, K_2CO_3, DMF, room temperature or 80 °C.

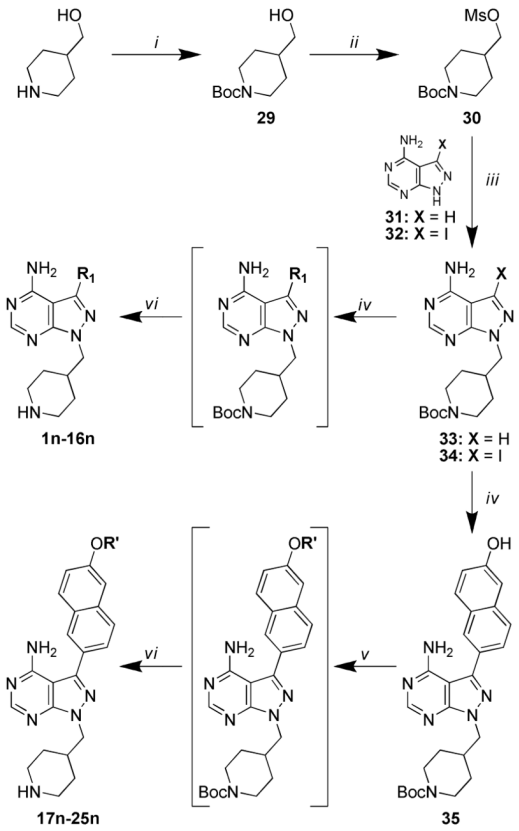

Scheme 2.

General synthetic procedures for compound series **n**. *i*) Boc_2O, CH_2Cl_2; *ii*) Methanesulfonyl chloride, TEA, CH_2Cl_2, 0 °C to room temperature; *ii*) Cs_2CO_3, DMF, room temperature or 80 °C; *iv*) Na_2CO_3, $Pd(PPh_3)_4$, boronic acid or boronate pinacol ester, H_2O/DME, 80°C; *v*) R′-halide, K_2CO_3, DMF, room temperature or 80 °C; *vi*) TFA/CH_2Cl_2.

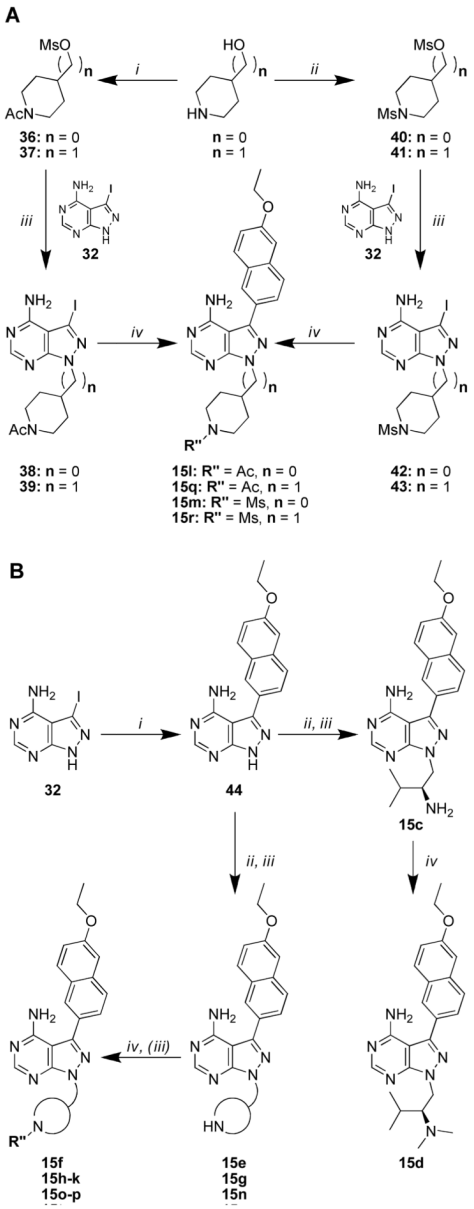

Scheme 3.

General synthetic procedures for compound series **15**. A) *i*) Ac_2O, TEA, CH_2Cl_2, then methanesulfonyl chloride; *ii*) Methanesulfonyl chloride, TEA, CH_2Cl_2; *iii*) Cs_2CO_3, DMF, 80 °C; *iv*) Na_2CO_3, $Pd(PPh_3)_4$, boronic acid or boronate pinacol ester, H_2O/DME, 80 °C in microwave. B) *i*) Na_2CO_3, $Pd(PPh_3)_4$, 6-ethoxynaphthalene-2-boronic acid, H_2O/DME, 110 °C; *ii*) Boc-R_2- OH, PS-PPh_3, DIAD, THF, room temperature to 70 °C; *iii*) TFA/CH_2Cl_2; *iv*) sodium methoxide in MeOH, then 2% AcOH, R″-aldehyde, $NaBH_3CN$.

Table 1

Enzymatic assay (IC_{50}) and *T. gondii* proliferation (EC_{50}) results for compounds with variable R_1 substructures (**1**-**25**) across the R_2 series **a**, **b**, and **n**. All results are the averages of at least three assays. Heat map representation of IC_{50} and EC_{50} results are presented in Tables 2AC.

Compound		Kinase Enzymatic IC_{50} (μM)			*T. Gondii* Proliferation EC_{50} (μM)
		*Tg*CDPK1	*Tg*CDPK1 (G128M)	SRC	
1	**b**	>5	>3	>10	>6.25
	n	>5	>3	>10	>6.25
2	**b**	0.0045	>3	0.13	0.23
	n	0.058	>3	>10	
3	**a**	0.019	>3	1.3	0.51
	b	0.0073	>3	0.58	0.041
4	**a**	0.040	>3	5.1	
5	**a**	0.0050	>3	0.65	0.080
	b	0.0041	>3	0.18	0.0030
	n	0.0022	>3	>10	1.7
6	**a**	0.012	>3	1.5	0.15
	n	0.081	>3	>10	
7	**a**	0.0091	>3	1.2	0.27
	n	0.018	>3	>10	>6.25
8	**a**	0.0036	>3	0.29	0.12
	b	0.013	>3	0.52	0.044
9	**b**	0.0025	>3	2.1	0.12
	n	0.0037	>3	>10	>6.25
10	**a**	0.13	>3	8.8	
	b	0.031	>3	2.2	
	n	0.015	>3	>10	2.2

Compound		Kinase Enzymatic IC_{50} (μM)			*T. Gondii* Proliferation EC_{50} (μM)
		*Tg*CDPK1	*Tg*CDPK1 (G128M)	SRC	
11	**a**	0.0050	>3	0.065	0.072
	b	0.0079	>3	0.12	0.35
	n	0.0025	>3	>10	0.63
12	**a**	0.024	>3	0.20	0.52
	n	0.018	>3	>10	>6.25
13	**b**	0.0031	>3	4.1	0.11
	n	0.0054	>3	>10	>6.25
14	**a**	0.0060	>3	0.67	0.021
	b	0.020	>3	2.0	0.010
	n	0.0049	>3	>10	0.41
15	**a**	0.0050	>3	0.38	0.018
	b	0.033	>3	2.2	
	n	0.0025	>3	>10	0.052
16	**n**	0.0034	>3	>10	0.058
17	**a**	0.010	>3	0.55	0.33
	n	0.0038	>3	>10	0.50
18	**a**	0.0006	>3	0.20	0.010
	n	0.0030	>3	>10	0.12
19	**a**	0.0032	>3	0.30	>6.25
	n	0.0026	>3	>10	0.16
20	**a**	0.0054	>3	0.26	0.31
	b	0.20	>3	1.1	
	n	0.0037	>3	>10	0.21
21	**a**	0.0009	>3	0.78	0.090
	n	0.0037	>3	>10	0.060

Compound		Kinase Enzymatic IC_{50} (μM)			*T. Gondii* Proliferation EC_{50} (μM)
		*Tg*CDPK1	*Tg*CDPK1 (G128M)	SRC	
22	**a**	0.0008	>3	0.041	0.0033
	n	0.0023	0.94	3.1	0.13
23	**a**	0.011	>3	0.28	0.14
	n	0.0013	>3	1.8	1.1
24	**a**	0.0055	>3	0.28	0.012
	n	0.0007	1.3	0.38	0.10
25	**a**	0.0040	>3	0.27	0.013

Table 2

A) Heat map representation of wild type *Tg*CDPK1 enzymatic IC_{50} values from Table 1. B) Heat map representation of SRC enzymatic IC_{50} values from Table 1. C) Heat map representation of wild type *T. gondii* proliferation EC_{50} values from Table 1. Blue represents compounds with desirable IC_{50} or EC_{50} values, transitioning to red for compounds with undesirable activities.

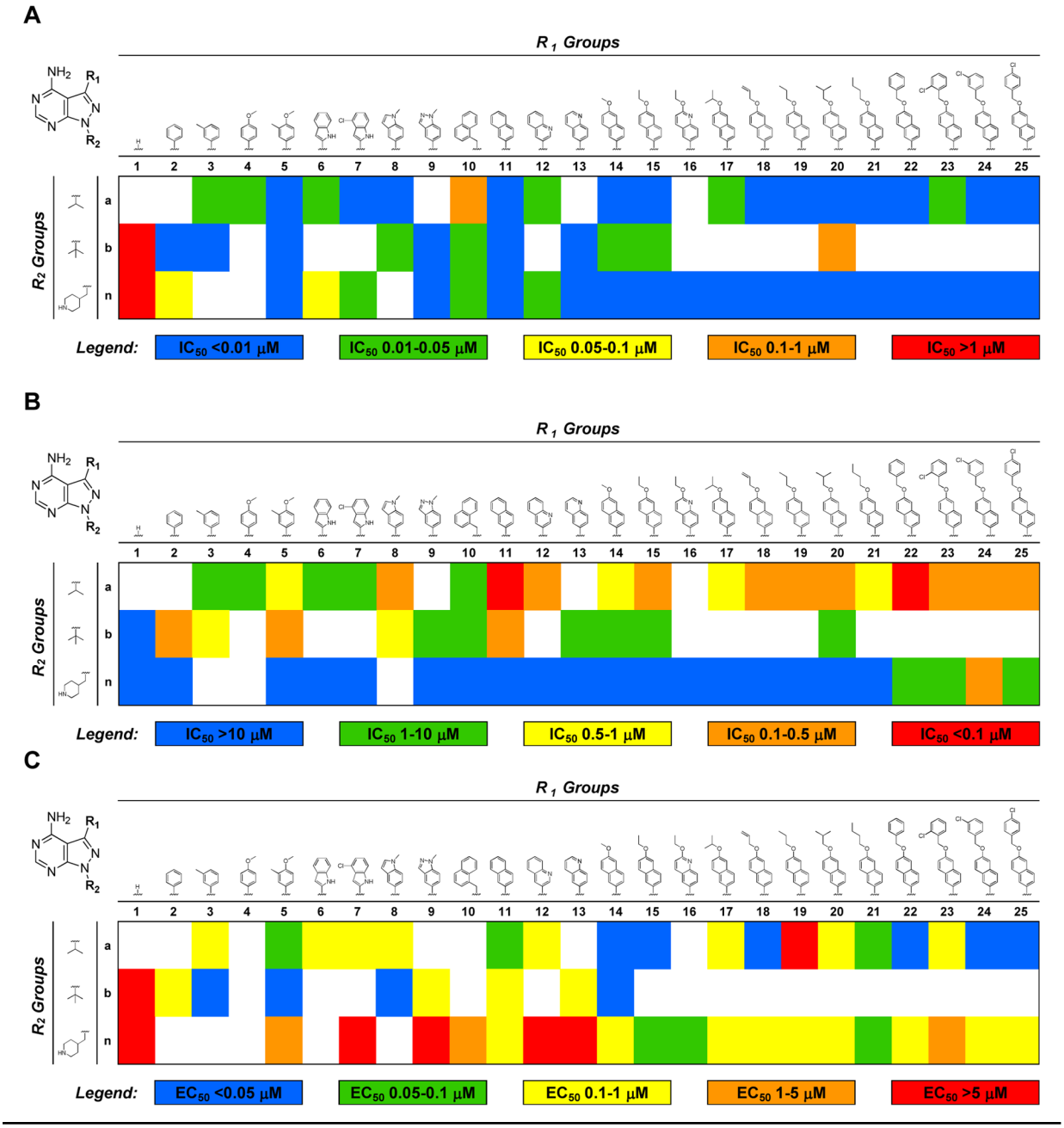

Table 3

Enzymatic assay (IC_{50}) and *T. gondii* proliferation (EC_{50}) results for compounds with variable R_2 (**a**-**w**) substructures and a 6-ethoxynaphthyl group (series **15**) at the R_1 position. All results are the averages of at least three assays.

	Kinase Enzymatic IC_{50} (μM)			
Compound 15-	***Tg*CDPK1**	***Tg*CDPK1 (G128M)**	**SRC**	***T. Gondii* Proliferation EC_{50} (μM)**
a	0.0050	>3	0.37	0.018
b	0.033	>3	2.2	
c	0.013	>3	>10	1.0
d	0.012	>3	>10	0.96
e	0.0091	>3	>10	0.97
f	0.0081	>3	>10	0.86
g	0.0026	>3	5.0	0.045
h	0.0024	2.6	5.6	0.050
i	0.0034	>3	8.7	0.090
j	0.0043	>3	>10	0.16
k	0.0043	0.98	0.73	0.34
l	0.0061	>3	1.6	0.029
m	0.0028	>3	0.81	0.035
n	0.0025	>3	>10	0.052
o	0.0029	>3	>10	0.14
p	0.0050	>3	>10	0.33
q	0.011	>3	>10	0.20
r	0.032	>3	>10	
s	0.0019	1.5	3.3	0.14
t	0.0022	1.4	5.2	0.049
u	0.0027	2.0	6.3	0.10
v	0.0030	2.9	6.7	0.18
w	0.0043	0.27	8.2	1.2

Table 4

Enzymatic assay results (IC_{50}) for an expanded panel of human kinases and growth inhibition (GI_{50}) of human cell lines. All results are the averages of at least three assays.

	Kinase Enzymatic IC_{50} (μM)								Human Cells GI_{50} (μM)	
Compound	***Tg*CDPK1**	**SRC**	**ABL**	**LCK**	**p38*α***	**EPHA3**	**CSK**	**EGFR**	**HL-60**	**CRL-8155**
14a	**0.0060**	0.67	0.82	0.079	>10	1.6	2.6	0.51	>10	>10
14n	**0.0049**	>10	>10	0.62	>10	>10	>10	>10	>10	>10
15a	**0.0050**	0.38	1.7	0.052	>10	3.7	3.1	0.70	>10	>10
15h	**0.0024**	5.6	>10	0.12	>10	>10	10	>10	>10	>10
15n	**0.0025**	>10	>10	0.96	>10	>10	10	>10	>10	>10
15o	**0.0029**	>10	4.6	3.3	>10	>10	>10	>10	>10	>10
16n	**0.0034**	>10	>10	>10	>10	>10	>10	>10	>10	>10